



Search for a New Heavy Gauge Boson W' with Electron+ \cancel{E}_T Event Signature

The CDF Collaboration
URL <http://www-cdf.fnal.gov>
(Dated: October 4, 2010)

We have searched for a new heavy charged vector boson, W' , decaying to an electron-neutrino pair in $p\bar{p}$ collisions at a center-of-mass energy of 1.96 TeV, using CDF II data corresponding to the integrated luminosity of 5.3 fb^{-1} assuming the standard model strength couplings. We found no evidence of this decay channel in the search results looking for an excess in the high mass region over standard model expectations, and thus set limits on the production cross section times branching fraction, assuming the neutrino from a W' boson decay to be light. If we assume the manifest left-right symmetric model, we exclude a W' boson with mass less than $1.1 \text{ TeV}/c^2$ at the 95% confidence level.

Preliminary Results

I. INTRODUCTION

Generically known the W' is a new charged heavy vector boson which is predicted in theories based on extensions of the gauge group of standard model, for example, left-right (LR) symmetric models [1]. The LR symmetric models can be also motivated as the intermediate step in grand unified theories [2] of the higher symmetry. In the models, the W' boson mass is obtained by the symmetry breaking in the right-handed electroweak gauge group of $SU(2)_R \times SU(2)_L \times U(1)_{B,L}$ [1], therefore they give natural explanations for the observation of suppression of $V + A$ currents in low energy weak processes. The produced W' in a $p\bar{p}$ collision can decay similarly to those of the standard model W boson but opens the $t\bar{b}$ channel if we assume the manifest left-right symmetry where the right-handed CKM matrix and the gauge coupling constant are identical to those of the standard model [3]. We select events that are consistent with the production of the standard model W boson decaying to an $e\nu_e$ final state on the standard model like but heavier object W' . We report the search results looking for an excess statistically in the high transverse mass (m_T) region and the limits on the relative rate to that of W boson to set a limit on the mass of the W' boson assuming the manifest LR symmetric model with the suppression of diboson decay modes [4].

II. DATA SAMPLE & EVENT SELECTION

We used a data sample of an integrated luminosity of 5.3 fb^{-1} of $p\bar{p}$ collisions at $\sqrt{s} = 1.96 \text{ TeV}$ recorded by the upgraded Collider Detector [5] at Fermilab (CDF II). The identified high E_T [6] electron of four-momentum is measured in the calorimeter and the neutrino can be detected by calculating missing transverse energy (\cancel{E}_T) which is derived from the momentum balance of all deposited energy in calorimeter. The CDF triggers require one electron candidate in the central electromagnetic calorimeter with transverse energy $E_T > 18 \text{ GeV}$ and a matching track with transverse momentum $p_T > 9 \text{ GeV}/c$. An additional trigger with $E_T > 70 \text{ GeV}$ and no restriction on the amount of energy leakage into the hadronic calorimeter was used to ensure high efficiency for high E_T electrons. Subsequently, we selected the candidate event sample by requiring an isolated electron candidate with $E_T > 25 \text{ GeV}$ and its track p_T greater than $15 \text{ GeV}/c$ in the fiducial region of the detector within $|\eta| < 1.0$. Additionally, dilepton events coming from Drell-Yan, $t\bar{t}$, and diboson backgrounds were removed. For the secondary electron, we select the electron E_T greater than 15 GeV in central or plug region. The QCD multijet events come from when one of the jets is misidentified as an electron and the missing energy from the vector sum of the transverse energy in the event satisfies $E_T > 25 \text{ GeV}$. In this case, the electron candidate E_T and \cancel{E}_T will less likely be comparable in magnitude, whereas a $W/W' \rightarrow e\nu_e$ event will have an electron and a neutrino going opposite direction with comparable magnitude in E_T and \cancel{E}_T , respectively, if p_T of the boson is much smaller than the mass of the boson. We require the candidate events to satisfy $0.4 < E_T/\cancel{E}_T < 2.5$. After all these selection cuts the transverse mass of a candidate event is calculated as

$$m_T \equiv \sqrt{2E_T\cancel{E}_T(1 - \cos\phi_{e\nu})}, \quad (1)$$

where $\phi_{e\nu}$ is the azimuthal opening angle between the electron candidate and the \cancel{E}_T direction. This m_T distribution has a Jacobian peak associated with the production and decay of the W boson as shown in Figure 1.

III. $W' \rightarrow e\nu$ SIGNAL

The $W' \rightarrow e\nu$ signal events are generated with PYTHIA [7] using CTEQ5L parton density functions (PDFs) [8] assuming that the right-handed sector CKM matrix and the $V + A$ couplings the strength are the same as that of left-handed sector of the standard model [3]. The W' boson with mass values of 500 to 1300 GeV/c^2 at 50 GeV/c^2 intervals were generated with 50 000 events at each mass values. We applied next-to-next-to-leading-order (NNLO) K-Factors [9] to the leading-order (LO) cross sections since the cross sections calculated with PYTHIA are in LO. The total acceptance times efficiency of the event selection cuts is obtained from 45% to 35% with decrease in above 800 GeV/c^2 W' boson. This is due to low efficiencies obtained by electron identification selection cuts for the very high energy electrons at more than 500 GeV . Figure 3 shows the generated W' boson mass distributions. The production of very heavy bosons on-shell is suppressed and distributes with large low mass tails due to the smallness of the PDFs at large momentum fraction of partons. The large tails in low mass regions also affect to drop the efficiency of the event selections with the cuts of electron $E_T > 25 \text{ GeV}$ and $\cancel{E}_T > 25 \text{ GeV}$ for the very high mass bosons in particular.

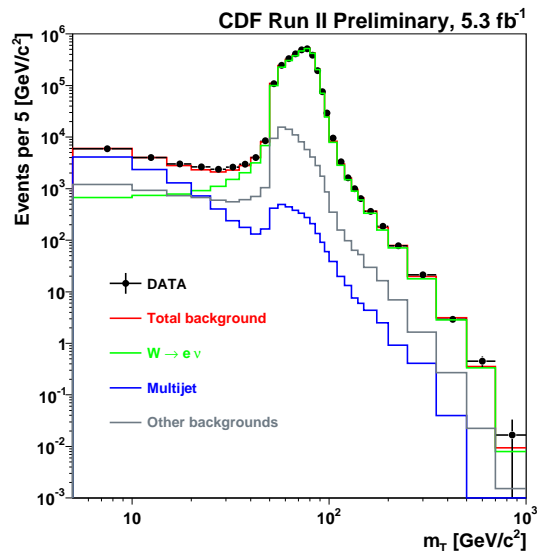


FIG. 1: The transverse mass distributions for $W/W' \rightarrow e\nu$ candidate events in 5.3 fb^{-1} of data and the standard model backgrounds.

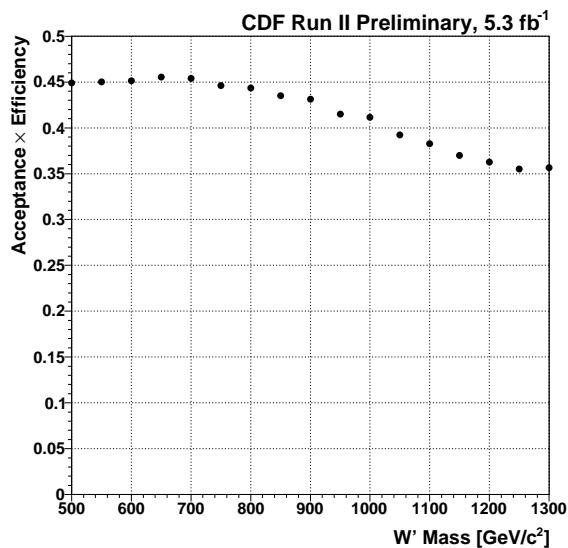


FIG. 2: Acceptance times event selection efficiency as a function of W' boson mass.

IV. BACKGROUNDS

Backgrounds to $W' \rightarrow e\nu$ signal production come from physics sources including real electrons in final state, such as $W \rightarrow e\nu$, $W \rightarrow \tau\nu \rightarrow eX$, $Z/\gamma \rightarrow ee$, $Z/\gamma \rightarrow \tau\tau \rightarrow eX$, $t\bar{t} \rightarrow eX$, Diboson (WW, WZ) $\rightarrow eX$, and from multijet background. The non-multijet backgrounds have been estimated using Monte Carlo (MC) samples which are generated with PYTHIA. We used theoretical cross section predictions for the expected background yields [9–11]. For multijet background estimation, we approached in data-driven. Since dijet events dominate multijet background, in the case of a jet being misidentified as an electron, it will be seen as recoiling against the other jets in the events. Therefore we expect to see back-to-back behaviour in the azimuthal opening angle between the primary electron candidate and vector summed E_T of all other jets, whereas $W/W' \rightarrow e\nu$ process does not have a strong correlation in the opening

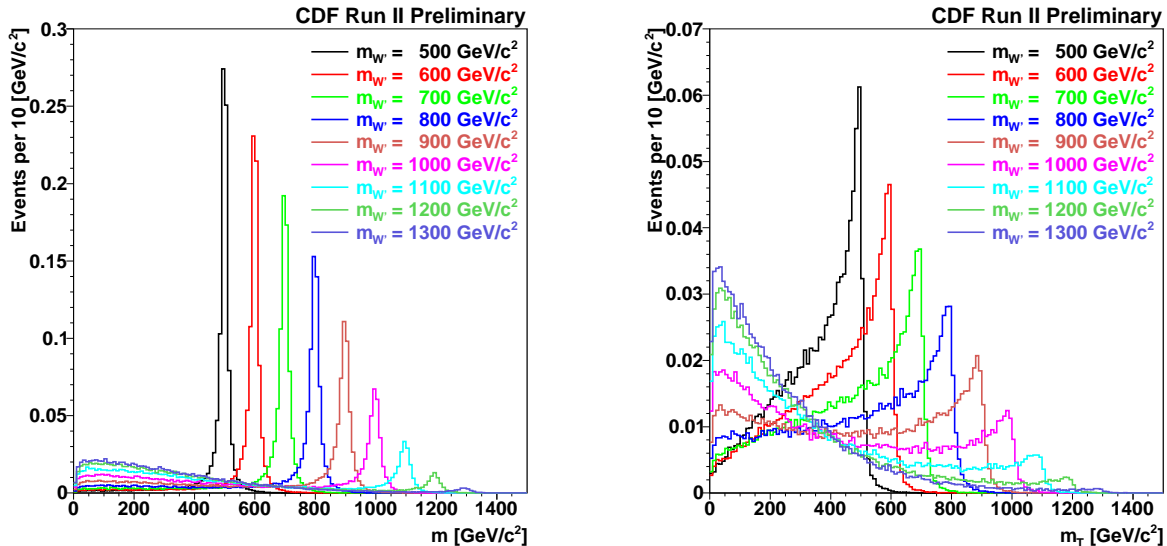


FIG. 3: The invariant mass (left) and transverse mass (right) distributions for $W' \rightarrow e\nu$ signal generated using PYTHIA.

angle. We used this different characteristics between $W/W' \rightarrow e\nu$ signal and QCD multijet in the azimuthal opening angle for the expectation calculation. The data and estimated background m_T distributions are compared in Figure 1. The contributions from $W \rightarrow e\nu_e$, QCD multijet, and the rest of the backgrounds above $m_T = 200 \text{ GeV}/c^2$ are listed in Table I.

V. SEARCH RESULTS

In order to estimate the size of the potential signal contribution in the sample, a binned maximum likelihood fit was performed on the observed m_T distribution between 0 and $1500 \text{ GeV}/c^2$, using the background predictions and the expected W' boson contribution with different mass values ranging from 500 to $1300 \text{ GeV}/c^2$. The fit results are shown in Table II, expressed as

$$\beta \equiv \frac{\sigma \cdot \mathcal{B}(W' \rightarrow e\nu_e)}{\sigma \cdot \mathcal{B}(W' \rightarrow e\nu_e)_{LR}}, \quad (2)$$

where the numerator is the observed cross section times branching fraction and the denominator is the expected from the manifest LR symmetric model. The expected signal yield was normalized by the observed W boson yield obtained from the fit, following the previous analysis technique in the recent search for $W' \rightarrow e\nu$ [12]. We found no statistically significant excess.

VI. SYSTEMATIC UNCERTAINTIES

Systematic uncertainties in the signal and background rates are considered on parton density functions (PDFs), electron energy scale, initial and final state radiation (ISR/FSR), jet energy scale, relative fractions of backgrounds, and multijet background. The most dominant contribution to the systematic uncertainties comes from the uncertainty in the PDFs. The total systematic uncertainty varies $\pm 5\%$ to $\pm 10\%$ for W' boson masses ranging from $m_{W'} = 500$ to $1300 \text{ GeV}/c^2$.

VII. LIMITS

We construct marginalized posterior probability distribution from the likelihood function where the systematic uncertainties were incorporated on the signals and backgrounds considering their correlation [13]. The 95% confidence

	Events in Each m_T Bins				
	200 - 250	250 - 350	350 - 500	500 - 700	700 - 1000
$W \rightarrow e\nu$	$712.52^{+49.66}_{-50.46}$	$355.31^{+24.76}_{-25.16}$	$85.14^{+5.93}_{-6.03}$	$13.32^{+0.93}_{-0.94}$	$0.48^{+0.03}_{-0.03}$
Multijet	$9.24^{+1.23}_{-0.25}$	$8.19^{+1.09}_{-0.22}$	$1.19^{+0.16}_{-0.03}$	$0.00^{+0.00}_{-0.00}$	$0.00^{+0.00}_{-0.00}$
Other Backgrounds	$69.78^{+6.81}_{-6.24}$	$32.94^{+3.46}_{-3.08}$	$8.12^{+0.87}_{-0.76}$	$0.90^{+0.11}_{-0.09}$	$0.09^{+0.01}_{-0.01}$
Total Backgrounds	$791.55^{+57.69}_{-56.95}$	$396.44^{+29.31}_{-28.46}$	$94.45^{+6.96}_{-6.82}$	$14.22^{+1.04}_{-1.03}$	$0.57^{+0.04}_{-0.04}$
Data	784	426	88	18	1

TABLE I: The binned likelihood fitting results using only background expectations. Shown are the expected numbers of background events in high m_T region above 200 GeV/ c^2 .

level limit in terms of β can be calculated by

$$0.95 = \frac{\int_0^{\beta_{95}} p(\beta) d\beta}{\int_0^{\infty} p(\beta) d\beta}, \quad (3)$$

where $p(\beta)$ is the marginalized posterior probability distribution. We set the 95% C.L. upper limit on the ratio of the observed cross section to the expected cross section assuming standard model strength couplings. We used the resulting likelihood function in only the “physical region” where this ratio is greater than or equal to zero. The obtained upper limits are summarized in Table II and plotted as a function of $m_{W'}$ in Figure 4. Using theoretical predictions assuming the manifest LR symmetric model, which has the right-handed CKM matrix and the gauge coupling constant identical to those of the standard model, these limits on the cross section times branching fraction were converted into limits on the mass of a W' boson. Here if we assume that W' boson has the standard model strength couplings, we can set the lower mass limit at the mass value at $\beta_{95} = 1$, which is where the cross section limit curve and the expected cross section with standard model strength curve cross. We take the lower bound of theoretical cross section to obtain the mass limit. Hence, the mass limit is found to be $m_{W'} > 1.1$ TeV/ c^2 .

VIII. CONCLUSION

We have performed a search for a new heavy charged vector boson decaying to an electron-neutrino pair with a light and stable neutrino in 1.96 TeV $p\bar{p}$ collisions. We do not observe any statistically significant excess over background expectations. We use a fit of the m_T distribution to set upper limits on the production and decay rate of a W' boson and exclude a W' boson with $m_{W'} < 1.1$ TeV/ c^2 at the 95% C.L., assuming the manifest LR symmetric model.

We thank the Fermilab staff and the technical staffs of the participating institutions for their vital contributions. This work was supported by the U.S. Department of Energy and National Science Foundation; the Italian Istituto Nazionale di Fisica Nucleare; the Ministry of Education, Culture, Sports, Science and Technology of Japan; the Natural Sciences and Engineering Research Council of Canada; the National Science Council of the Republic of China; the Swiss National Science Foundation; the A.P. Sloan Foundation; the Bundesministerium für Bildung und Forschung, Germany; the World Class University Program, the National Research Foundation of Korea; the Science and Technology Facilities Council and the Royal Society, UK; the Institut National de Physique Nucleaire et Physique des Particules/CNRS; the Russian Foundation for Basic Research; the Ministerio de Ciencia e Innovación, and Programa Consolider-Ingenio 2010, Spain; the Slovak R&D Agency; and the Academy of Finland.

-
- [1] J.C. Pati and A. Salam, Phys. Rev. D **10**, 275 (1974); R.N. Mohapatra and J.C. Pati, Phys. Rev. D **11**, 566 (1975); *ibid.* Phys. Rev. D. **11**, 2558 (1975); G. Senjanovic and R.N. Mohapatra, Phys. Rev. D **12**, 1502 (1975).
[2] P. Langacker, Phys. Rep. **72**, 185 (1981); H. Georgi, *Particles and Fields*, edited by C. E. Carlson (AIP, New York, 1975), p. 575; H. Fritzsch and P. Minkowski, Ann. Phys. (N.Y.) **93**, 193 (1975).
[3] This is called manifest left-right symmetric model For detail discussion, See A. Masjero, R. N. Mohapatra, and R. Peccei. Nucl. Phys. B 192, 66 (1981); J. Basecq *et al.*, Nucl. Phys. B 272, 145 (1986).
[4] G. Altarelli *et al.*, Z. Phys. C **45**, 109 (1989).

TABLE II: The expected numbers of events from $W' \rightarrow e\nu_e$ process, N_{exp} , assuming the manifest LR symmetric model and normalized by the observed W boson yield. We also show the observed relative rate of the W' boson production from the fit described in the text, and the 95% C.L. upper limit on this relative rate. The uncertainties are statistical only and do not include systematic uncertainties. The 95% upper limits include both statistical and systematic uncertainties.

$m_{W'}$ GeV/ c^2	N_{exp} (events)	$\beta \left(= \frac{\sigma \cdot \mathcal{B}(W' \rightarrow e\nu_e)}{\sigma \cdot \mathcal{B}(W' \rightarrow e\nu_e)_{LR}} \right)$ Fit ($\times 10^{-2}$)	Upper Limit
500	5828	$0.066^{+0.220}_{-0.066}$	6.02×10^{-3}
550	3407	$0.178^{+0.258}_{-0.178}$	7.88×10^{-3}
600	2037	$0.269^{+0.364}_{-0.269}$	1.10×10^{-2}
650	1218	$0.451^{+0.543}_{-0.451}$	1.68×10^{-2}
700	731	$0.551^{+0.771}_{-0.551}$	2.39×10^{-2}
750	433	$0.490^{+0.955}_{-0.490}$	3.12×10^{-2}
800	263	$0.518^{+1.33}_{-0.518}$	4.28×10^{-2}
850	160	$0.723^{+1.89}_{-0.723}$	6.38×10^{-2}
900	100	$1.06^{+2.90}_{-1.06}$	9.96×10^{-2}
950	62	$1.69^{+4.86}_{-1.69}$	1.68×10^{-1}
1000	41	$2.16^{+8.10}_{-2.16}$	2.84×10^{-1}
1050	27	$2.81^{+14.6}_{-2.81}$	5.16×10^{-1}
1100	19	$2.41^{+26.4}_{-2.41}$	9.30×10^{-1}
1150	14	$3.61^{+48.7}_{-3.61}$	1.76
1200	10	$10.3^{+87.8}_{-10.3}$	3.21
1250	8.1	$29.8^{+139}_{-29.8}$	5.19
1300	6.7	$80.9^{+217}_{-80.9}$	8.12

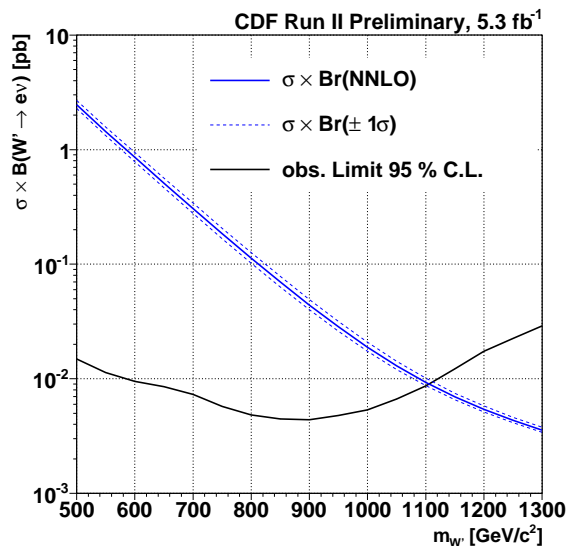


FIG. 4: The 95 % C.L. limits on cross section times branching fraction as a function of W' mass. The region above the curve is excluded at the 95 % C.L. Also, the cross section times branching fraction assuming the standard model strength couplings, $\sigma \cdot \mathcal{B}(W' \rightarrow e\nu)_{LR}$, is shown along with its uncertainty. The intercept of the cross section limit curve and the lower bound of the theoretical cross section yields $m_{W'} > 1.1 \text{ TeV}/c^2$ at the 95 % C.L.

[5] D. Acosta *et al.* (CDF Collaboration), Phys. Rev. D **71**, 032001 (2004).

[6] We use a coordinate system where θ is the polar angle to the proton beam, ϕ is the azimuthal angle about the beam axis, and η is the pseudorapidity defined as $-\ln(\tan(\theta/2))$. Energy (track momentum) measured transverse to the beam line is denoted as E_T (p_T).

[7] T. Sjostrand *et al.*, Comput. Phys. Commun. **135**, 238 (2001).

[8] H. L. Lai *et al.* (CTEQ Collaboration), Eur. Phys. J. C **12**, 375 (2000).

- [9] R. Hamberg, W. L. van Neerven, and T. Matsuura, Nucl. Phys. B **39**, 343 (1991); **644**, 403 (E) (2002).
- [10] J. M. Campbell and R. K. Ellis, Phys. Rev. D **60**, 113006 (1999).
- [11] M. Cacciari *et al.*, J. High Energy Phys. **0404**, 068 (2004); N. Kidonakis and R. Vogt, Phys. Rev. D **68**, 114014 (2003).
- [12] A. Abulencia *et al.* (CDF Collaboration), Phys. Rev. D. **75**, 091101 (2007).
- [13] MClimit code (<https://plone4.fnal.gov:4430/P0/phystat/packages/0711001>), Tom Junk, CDF Note 8128, and Joel Heinrich, CDF Note 7587